Efficient and Comfortable Haptic Retargeting with Reset Point Optimization

Aoxin Sun, Jian Wu, Runze Fan, Sio Kei Im, Lili Wang

***Abstract*—Passive haptics utilize the shape of a physical object to convey feedback to the user and enhance immersion in virtual reality. Haptic retargeting is a passive haptic interaction method. Its mapping of physical objects to virtual objects solves the matching problem between virtual and physical objects in the passive haptic method. However, most existing haptic retargeting methods improve efficiency without considering the important factor of user comfort. In this paper, we propose an efficient and comfortable haptic retargeting method based on reset point optimization. First, we construct two maps indicating user interaction comfort: the RULA score map and the dominant hand gain map. Subsequently, we propose a reset point optimization algorithm based on these two maps. Moreover, we also optimize the selection of the physical proxy and the placement location when the reset occurs. The user study results show a significant improvement in the efficiency and comfort of our method compared to state-of-the-art methods.**

***Index Terms*—Virtual reality, haptic retargeting, ergonomics, psychology, reset techniques.**

I. Introduction

With the rapid development of computer software and hardware, virtual reality (VR) technology has been practically applied in many aspects. Many fields have gradually integrated VR technology, such as healthcare, education, and entertainment. When a user tries to manipulate a virtual object in a VR environment, the absence of haptic feedback can greatly reduce the user's sense of immersion. Passive haptic technology solves this problem well. It utilizes physical proxies to convey feedback to the user through their shape, thus giving tangible dimension to virtual objects. Traditional passive haptic techniques require one-to-one correspondence between physical proxies and virtual objects, which has high requirements for physical scenes. To solve this problem, haptic retargeting is proposed. This technique can provide passive haptic feedback to the user by mapping multiple virtual objects to physical proxies by deceiving human perception. Previous haptic retargeting methods can be divided into two categories. The first category of methods focuses on static virtual scenes. These methods use only one physical proxy, and they redirect the user's hand to this physical proxy when the user touches a virtual object in the virtual scene [1]. The second class of methods has multiple physical proxies, and they consider the distribution or shape of the physical proxies and the virtual object and choose one of the props to represent the virtual object that the user wants to touch [2], [3]. This type of method focuses on dynamic virtual scenes. It allows virtual objects to move to other locations in the virtual world. Our haptic retargeting method belongs to the second category of methods, providing users with more freedom of interaction and good experience.

In haptic retargeting methods, when the user performs hand retargeting continuously, the cumulative offset between the virtual hand and the real hand becomes gradually larger. In general, haptic retargeting methods set a fixed threshold. When the offset exceeds the threshold, the user will perceive the gap between the virtual hand and the physical hand, greatly affecting user's immersion, and a reset operation is required to align the virtual hand with the physical hand to remove the offset. How to set a reasonable reset position to improve user experience has been an important problem. The most common method is to set the reset point at a fixed location [1], [4], [5]. However, this method often results in excess hand movement and is inefficient. To improve efficiency, many researchers have explored reset techniques. Ziming et al. [4] proposed a haptic retargeting method based on proxy importance that can reduce the number of resets. Matthews et al. [6] proposed an adaptive reset method. It reduces the user's hand movement by dynamically changing the reset point position. However, user comfort is one of the most important indicators for evaluating the goodness of an interaction system, and only comfortable interactions can make it possible for users to use VR applications for a long time. User comfort includes postural comfort and psychological satisfaction, which correspond to ergonomics and psychology, respectively. None of these methods take user comfort into account.

In this paper, we propose a new haptic retargeting pipeline based on our reset point optimization method. When a reset occurs, our method can perform reset optimization. First, we construct two maps, the RULA (rapid upper limb assessment) score map (RSM) and the dominant hand gain map ($DHGM$), which are closely related to the comfort of user interaction. Based on these two maps, we propose a reset point optimization algorithm. Moreover, we further optimize the selection of the physical proxy and the placement location when the reset occurs. Finally, we designed a user study to compare our method with the state-of-the-art haptic retargeting reset optimization methods. The user study results show a significant improvement in the efficiency and comfort of our method compared to Ziming et al.'s method [4] and Matthews et al.'s method [6].

Fig. 1 shows a user using our method for haptic retargeting. The image on the left shows the 3PP. A right-handed user is

Aoxin Sun, Jian Wu, Runze Fan, and Lili Wang are with State Key Laboratory of Virtual Reality Technology and Systems, School of Computer Science and Engineering, Beihang University, Beijing, 100191 and Peng Cheng Laboratory, Shenzhen, Guangdong, China, 518000.

Sio Kei Im is with Macao Polytechnic University, Macao, China, 999078.

Lili Wang is the corresponding author: wanglily@buaa.edu.cn

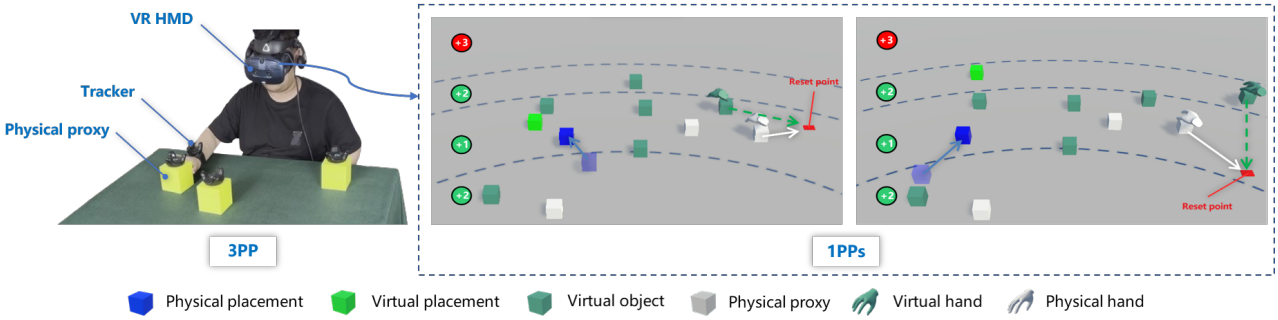

Fig. 1. User performs haptic retargeting using our method. The left image shows the 3PP (Third-Person Perspective). The right images show the 1PPs (First-Person Perspective) in VR. The two images on the right side have different reset point positions due to the different distribution of virtual objects. Even though the physical proxies are all placed in the same position as in the left image, the optimized reset points are different.

wearing a VR HMD on his head with a tracker attached to his right wrist. Three yellow cubes with trackers are physical proxies. The two images on the right show the user's 1PPs in VR. The blue dotted lines on the virtual plane represent the areas divided by different RULA scores, and the specific scores are labeled on the left side of the images. A lower score indicates a higher level of user comfort. We visualized the three physical proxies in white for better illustration, and the user cannot see them in 1PP. As shown in the two images on the right, the user needs to perform a reset operation. The user needs to take the physical proxy to the reset point to perform the reset operation, and then place the physical proxy to the specified placement location. The difference between these two images is the distribution of virtual objects. Even though the distribution of physical proxies is the same, the reset point positions optimized by our method are different, and both are set in the area with the lowest RULA score and on the side of the user's dominant hand. Moreover, the placement locations have also been updated to more reasonable and comfortable positions (From light blue cube to dark blue cube. The light blue cube is the original physical placement, and the dark blue cube is the new physical placement calculated by the algorithm.)

In summary, the main contributions of our work are as follows:

- we propose a new haptic retargeting pipeline based on reset point optimization, which introduces for the first time the influence of ergonomics and psychology in the retargeting technique;
- we propose a reset point optimization method based on the RULA score map and dominant hand gain map;
- We propose a physical proxy and placement location updating method when a reset occurs;
- Through user study we find that our method improves user efficiency and comfort.

The rest of the paper is organized as follows: First, we review previous haptic retargeting methods in Section II. Then, we give the design rationale of our method in Section III. We detail our method in Section IV and obtain key parameters through a pilot user study in Section V. Then we evaluate our method through a user study in Section VI. Finally, we discuss the superiority, limitations, and possible future improvements of our method in Section VII.

II. Related Work

In this section, we review existing haptic retargeting methods in VR and reset techniques in haptic retargeting.

A. Haptic Retargeting

Haptic technologies in virtual reality can be categorized into two main groups: active haptic and passive haptic. Active haptic technologies use special devices with small motors to provide vibrotactile feedback when touching virtual objects in the scene [7]–[9]. Passive haptic is an interaction method in virtual reality proposed by Insko et al [10]. It utilizes physical proxies to convey feedback to the user through their shapes, thus giving tangible dimensions to virtual objects. Passive haptics technology integrates low-fidelity physical proxies into high-fidelity visual virtual environments, which greatly enhances the sense of presence and improves the transfer of spatial knowledge training. However, passive haptic technology application has certain limitations. Passive haptic techniques need to fulfill the similarity and colocation criterion [11] for proxy-based haptics, i.e., virtual objects and physical proxies must correspond in position and shape, which has high requirements for the real scene when the real scene space or the number of physical proxies is limited; passive haptic technology will be ineffective. The researchers proposed haptic retargeting technology for this problem.

Gibson et al. [12] pointed out that observers rely more on information obtained through vision than information obtained through haptics when visual and haptic information conflict. Burns et al. [13] investigated the difference in users' sensitivity to two types of visual feedback when touching a virtual object, namely, hand approaching the virtual object and hand going deeper into the virtual object, and found that users were more sensitive to the latter case than to the former case. Based on these theories, Azmandian et al. [1] first proposed haptic retargeting in 2016, where they proposed three warping techniques: body warping, world warping, and hybrid warping, which maps multiple virtual objects onto one physical proxy.

Since then, many researchers have explored haptic retargeting techniques in greater depth. Matthews et al. [5] proposed an interface warp based on Azmandian's work. This method produces warping that acts on the virtual interface rather than the user's hand. They [14] also proposed a remapping interface system that utilizes haptic retargeting techniques to reuse a limited set of controls for various interfaces. The system can create virtual user interfaces that adapt to the environment in

which they are used and provide accurate haptic feedback. Zenner et al. introduced Blink Suppression Hand Redirection (BSHR) [15], which momentarily moves the virtual hand when the user's vision is suppressed when blinking. They also combined this method with saccadic redirection and introduced Saccadic & Blink-Suppressed Hand Redirection (SBHR) technique [16]. Montano et al. [17] proposed the Erg-O, which defined two spatial partition trees to make user interaction more comfortable. Simeone et al. [18] explored the concept of Substitutional Reality in the context of Virtual Reality. Every physical object surrounding a user is paired, with some degree of discrepancy, to a virtual counterpart. De et al. [19] proposed an algorithm that analyzes the available tangible and virtual objects to find the best grasps in terms of matching haptic sensations. To provide finer passive haptic feedback, some researchers have developed special devices for haptic retargeting. Cheng et al. [2] proposed Sparse Haptic Proxy in haptic retargeting. They designed a hemispherical physical proxy capable of providing haptic proxies at different angles on the surface of a virtual object through haptic retargeting. Yang et al. [20] created a VR gripper shaped like chopsticks and proposed the Ungrounded Haptic Retargeting technique. This interaction technique provides a realistic haptic experience for the grasping tool using only passive mechanisms. Huang et al. [21] used a motorized turntable that rotates the correct haptic device to the right direction at the right time to match what users are about to touch. VRHapticDrones [22] is a system utilizing quadcopters as levitating haptic feedback proxy. It can provide unintrusive, flexible, and programmable haptic feedback in virtual reality. Abtahi et al. [23] proposed HoverHaptics, an autonomous safe-to-touch quadcopter and its integration with a virtual shopping experience. In addition, many researchers have integrated haptic retargeting techniques with AI technologies to improve interaction freedom. Clarence et al. [24] explored software-based reach prediction as a means of facilitating responsive, unscripted retargeting. They trained a Long Short-Term Memory network on users' reach trajectories to predict intended targets. Salvato et al. [25] proposed a technique for predicting when a user will start interacting with a virtual object by touch before the user starts interacting with the virtual object. They used a time series of tracked hand poses, along with virtual object geometry to perform the prediction.

Previous haptic retargeting methods include methods that support a single proxy for static scenes, methods that support multiple proxies for dynamic scenes, and methods that use customized devices. Our method belongs to the methods that support multiple proxies for dynamic scenes, which has a wider range of application scenarios.

B. Reset Techniques

In haptic retargeting, when the user performs hand retargeting continuously, the cumulative offset between the virtual hand and the real hand becomes gradually larger. When the offset exceeds a fixed threshold, a reset operation is required. After receiving a prompt that a reset is needed, the user moves the virtual hand to a reset point or a reset region where the virtual hand and the real hand are aligned. There is a lot of research going on to make the reset interaction easier or to reduce the number of resets.

Feick et al. [26] investigated the use of physiological and interaction data to detect movement discrepancies between a user's real and virtual hand. It is a new approach to identify discrepancies which are too large and therefore can be noticed. Zhao et al. [27] proposed a spatial warping method based on functional optimization that allows users to touch complex shapes without introducing resets. This method also allows continuous retargeting between two virtual objects that do not share the same physical proxies without the need for a reset. Yang et al. [28] proposed that when guiding users to place virtual objects, physical proxies can be placed at the location closest to the sum of the distances to multiple other virtual objects, thus reducing the reset probability. Matthews et al. [5] asked the user to touch a nearby physical button between retargeting interactions to force a reset of the virtual hand's position so that the user did not need to move the hand far away to perform the reset operation. They [3] also investigated how to combine gaze-point-based user-selected target prediction with multi-physics prop mapping and on-the-fly retargeting techniques to minimize resets. Matthews et al. [6] also proposed an adaptive reset technique so that each reset occurs at an optimal location. This method determines the reset point within the redirection path based on factors such as offset thresholds and minimized hand movement, thus reducing additional hand movement. Ziming et al. [4] proposed a haptic retargeting method based on proxy importance, which calculates the proxy importance of props to select more reasonable physical proxies and placement locations. The results show that the method can greatly reduce the number of resets.

Previous reset techniques, while capable of reducing the reset distance or the number of resets, still have many shortcomings. Some methods have limited application scenarios and are not easily scalable. Some methods are not reasonable for the reset point location, which may lead to additional hand movement. In addition, user comfort is an important indicator of how good a human-computer interaction system is, and many previous retargeting methods do not take this factor into account. Our method improves efficiency while taking into account the user's ergonomic and psychological needs so that the user can complete the interaction task comfortably and efficiently.

III. Design Rationale

We aim to design a dynamic reset points optimization method for haptic retargeting that improves task completion efficiency and meets the ergonomic and psychological needs of the user so that the user can use haptic retargeting efficiently and comfortably. In this section, We will introduce the design rationale of our method in the following aspects.

A. Perception

When users use a haptic retargeting method, the magnitude of the retargeting gain can significantly impact their perception. If the retargeting gain is too large, the user will perceive the gap between the virtual hand and the physical hand [29]–[32]. There are two types of retargeting gains: angular gain G_A

and translation gain G_T. The angular gain G_A is computed using the relative angle between the physical and virtual path vectors, and the translational gain G_T is the ratio between the lengths of the two vectors.

Zenner et al. [29] found that when $G_A < 4.5°$ and $0.88 < G_T < 1.07$, the user is unable to distinguish the difference between the real hand and the virtual hand and is unable to perceive the redirection. However, Ziming et al. [4] demonstrated through user study that a small threshold will increase the number of resets, thus seriously affecting the user experience. Clarence [30] et al. investigated the limits of haptic retargeting that people can withstand when performing haptic retargeting. Conducting experiments with up to 30° of offset, the researchers determined the overall limits of haptic retargeting and found that a physical proxy could be remapped to a virtual object up to $16.14°$.

Based on the above works, it is easy to see that a smaller retargeting gain threshold will make the difference almost imperceptible to the user, resulting in a better usage experience. A larger retargeting gain threshold provides a greater range of virtual hand manipulation, thus reducing the number of resets. To balance the user experience and the interaction range, inspired by previous work [4], [6], we set the angular gain threshold A to $15°$ and the translation gain threshold T to $[0.83, 1.2]$. We also consider the effect of retargeting gain when setting the reset point and updating the proxy and placement location as a way to improve the user experience.

B. Ergonomics and Psychology

Many works of human-computer interaction only focus on factors such as efficiency and accuracy, and neglect the important issue of user comfort. Whether users can satisfy their ergonomic and psychological needs while using an interactive system will directly affect their experience.

RULA [33] is a survey method developed for use in ergonomics investigations of workplaces where work-related upper limb disorders are reported. This tool requires no special equipment to provide a quick assessment of the postures of the neck, trunk, and upper limbs, along with muscle function and the external loads experienced by the body. We will use RULA in our method to assess user comfort and use this to optimize the position of the reset point for haptic retargeting.

In addition, psychological works [34], [35] suggest that people prefer to touch or move objects on the side of their dominant hand. Casasanto et al. [34] found that right- and left-handers implicitly associate positive ideas like "goodness" and "honesty" more strongly with their dominant side of space, the side on which they can act more fluently, and negative ideas more strongly with their non-dominant side. Daini et al. [35] designed a manual line bisection task, and results show a rightward bias when right-handed individuals bisect lines using their right hand. Rowe et al. [36] found that the motor system can be activated quickly when the object is on the dominant-hand side. We will consider this when optimizing the reset point's position, placing it at the user's dominant-hand side.

C. Efficiency

Efficiency has always been an important indicator of an interactive system's performance. Users want to spend less effort and time completing interaction tasks. Haptic retargeting methods generally consist of three tasks: picking up the virtual object, placing the virtual object, and resetting when the gain exceeds a threshold. The hand movements resulting from the first two tasks are limited by the retargeting technique itself [1] and do not easily lend them to optimization.

To improve the efficiency of haptic retargeting, current methods have tried to reduce the number of resets or optimize the distance from the reset point to the user's hand [4], [6]. Ziming et al. [4] proposed a haptic retargeting method based on proxy importance calculation to reduce the number of resets. Matthews et al. [6] proposed an adaptive reset method to reduce hand movement. Inspired by previous work, we used the framework of proxy importance based haptic retargeting method [4] in selecting physical proxies and placement locations to reduce the number of resets, and we also optimized the reset point location so that the reset point appears near the user's hand when reset is needed.

IV. Method

In this section, we will introduce the implementation of our method. Fig. 2 shows the pipeline of our haptic retargeting method. Standard haptic retargeting generally consists of two main steps: picking up the virtual object with haptic retargeting and placing the virtual object with haptic retargeting. In both steps, a threshold detection is performed. When the retargeting gain exceeds the threshold, the current haptic retargeting interaction is stopped, and a reset is inserted. When a reset occurs, our reset point optimization method will be used. First, we construct two comfort maps(Section IV-A). Then, we grid the virtual desktop and initialize candidate reset points(Section IV-B). Next, we determine the reset point locations through algorithmic optimization(Section IV-C). Finally, we update the proxy or placement location(Section IV-D).

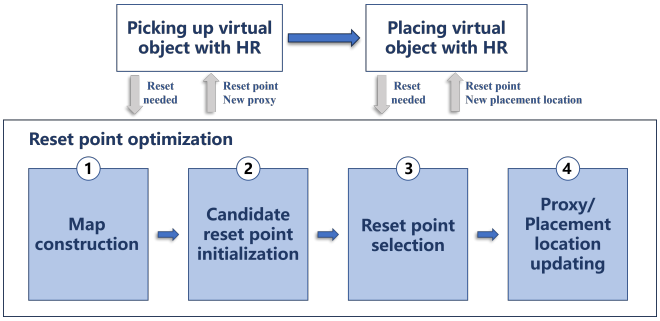

Fig. 2. Pipeline of our reset point optimization based haptic retargeting method.

A. Comfort Maps Construction

We first introduce the construction of comfort maps, including the RULA score map and dominant hand gain map, which indicate the user's comfort level when performing haptic retargeting.

1) RULA score map

RULA [33] can measure comfort in many parts of the human body, such as the neck, arms, and legs. For haptic

retargeting methods, the part of the body that undergoes frequent movements is the arm, so we mainly use the lower arm score of RULA to measure the user's comfort level. Other parts of the body that are not related to the haptic retargeting method and are not amenable to quantitative analysis are not considered in our method. The lower arm score is shown in Fig. 3a, +1 score for 60-100° flexion, +2 score for less than 60° or more than 100° flexion.

Based on the RULA lower arm score, we constructed the RULA score map $RSM(x, y)$ shown in Fig. 3b, which is used to indicate the user's postural comfort level at different positions of the hand. (x, y) denotes the position of the user's real hand on the desktop. The value of $RSM(x, y)$ indicates the comfort score of the user's posture when the hand is in (x, y) position. A lower score indicates a higher level of user comfort. The difference in angle between Fig. 3a and Fig. 3b is due to the different datum. The angle in Fig. 3a is the flexion angle of the arm. For ease of calculation, we convert the flexion angle to the angle between the upper and lower arm, +1 score for 80-120°, +2 score for less than 80° or more than 120° (calculated from $180° - 100° = 80°$ and $180° - 60° = 120°$, $60°$ and $100°$ are the elbow flexion-extension cut-off angles for the RULA lower arm score).

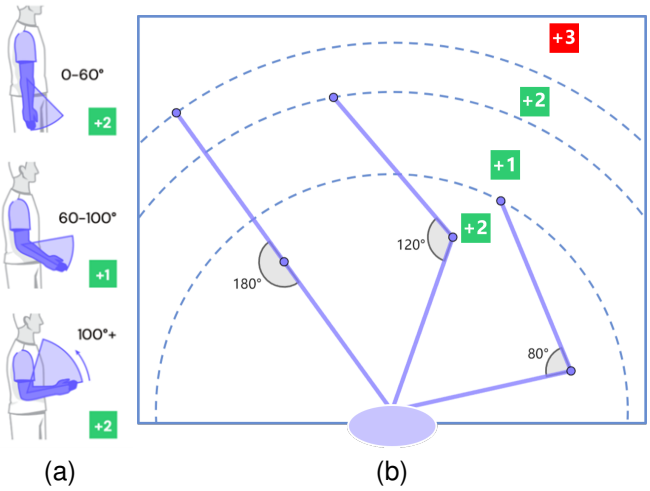

Fig. 3. (a) Lower arm score of RULA; (b) The construction of RULA Score map. Different scores indicate different comfort levels, with lower indicating more comfort. The purple ellipse indicates the position of the user's body, and the purple folded line indicates the user's arm.

In general, the length of the lower arm plus the length of the hand is approximately equal to that of the upper arm, and the average arm length of a normal person is 65-75cm [37], [38]. In our method, we abstract the human arm as two equal-length line segments, which are connected by an axis of rotation (a.k.a. the elbow joint). The score division of RSM is derived from the equation(1):

$$RSM(x,y) = \begin{cases} +2 & r < l \cdot \sin(80°/2) \\ +1 & l \cdot \sin(80°/2) < r < l \cdot \sin(120°/2) \\ +2 & l \cdot \sin(120°/2) < r < l \\ +3 & r > l \end{cases} \tag{1}$$

where r denotes the distance from the user's hand position (x, y) to the body, l denotes the arm length (taken as 70 cm in our method).

Moreover, we defined an additional +3 score area, which is the area that cannot be touched when the arm is fully extended. The user has to get up and bend at the waist, etc., to touch the area, which is considered to cause great discomfort to the user, so the score is set to the highest. In addition, the elbow flexion angle is not easy to measure when the user is performing the interaction task, while our area division method only needs to calculate the approximate distance from the user's hand to the body in order to judge whether the user's lower arm movement meets the ergonomic requirements.

2) Dominant hand gain map

According to related psychological work [34]–[36], we would like to set the reset point on the side of the user's dominant hand as much as possible when setting the reset point, e.g., if a right-handed user is using our haptic retargeting method. When it is necessary to reset, we will set the reset point on the right side of the user's current real hand position. This method of setting the reset point is more in line with people's psychological expectations.

Based on this, we construct the dominant hand gain map $DHGM(x, y)$ shown in Fig. 4 to indicate the psychological comfort level of the user's hand as it moves to different positions. (x, y) denotes the position to which the user will move his hand. The value of $DHGM(x, y)$ indicates the psychological comfort level of the user's hand movement when moving to the reset point position (x, y). A lower score indicates a higher level of user psychological comfort.

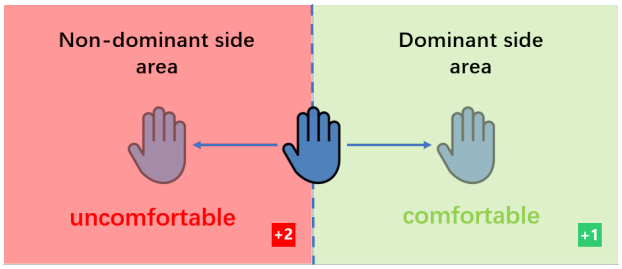

Fig. 4. The construction of dominant hand gain map. The desktop is divided into the dominant side area and the non-dominant side area based on the user's hand position. Different scores indicate different psychological comfort levels, with lower indicating more comfort.

We divide the desktop into two areas based on the location of the user's hand when reset occurs: the dominant side area and the non-dominant side area. The score division of $DHGM$ is derived from the equation(2):

$$DHGM(x,y) = \begin{cases} +1 & \text{in dominant side area} \\ +2 & \text{in non-dominant side area} \end{cases} \tag{2}$$

We evaluate reset points by considering the dominant hand gain value α to make it easier to set the reset point on the user's dominant hand side. α is a value less than 1, which makes candidate reset points in the dominant side area more likely to be selected. It will be determined by user study in Section V, and its role will be introduced in Section IV-C.

B. Candidate Reset Point Initialization

Our haptic retargeting method is to move the cube block on a 1.5m*1.5m desktop, and the virtual objects will be randomly

distributed on virtual planes of equal size. As shown in Fig. 5, we grid the virtual plane and place a candidate reset point of size 0.1m*0.1m every 0.15m, totaling 9*9=81 candidate reset points. Such a setup makes the distance between neighboring reset points at most 0.2m and covers almost the whole virtual plane. It greatly simplifies the optimization of reset points.

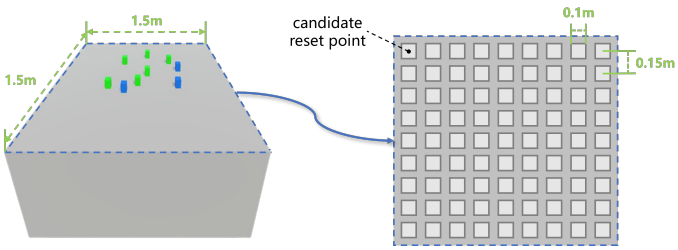

Fig. 5. The left side of the figure shows our virtual desktop, which is 1.5m*1.5m. As shown on the right side of the figure, we grid the virtual desktop to set the candidate reset points.

C. Reset Point Optimization Algorithm

Based on the comfort maps and candidate reset points described above, we propose a reset point optimization algorithm. The algorithm is shown in Algorithm 1. Given Angle threshold A, Translation threshold T, Candidate reset points $RList$, Physical hand position H_p, Virtual hand position H_v, and dominant hand gain α, the final score for each candidate reset point S is calculated.

Algorithm 1 Reset point optimization algorithm based on comfort maps

Input: Angle threshold A, Translation threshold T, Candidate reset points $RList$, Physical hand position H_p, Virtual hand position H_v, dominant hand gain α
Output: Final score for each candidate reset point S

1: $RList' \leftarrow removeCollision(RList)$
2: **for** *each* r *in* $RList'$ **do**
3: $S_R(r) \leftarrow RSM(r)$
4: $S_D(r) \leftarrow getDistance(H_p, r)$
5: $S_G(r) \leftarrow getRetargetingGain(A, T, H_p, H_v, r)$
6: **end for**
7: **for** *each* r *in* $RList'$ **do**
8: $S_R(r) \leftarrow S_R(r)/max(S_R)$
9: $S_D(r) \leftarrow S_D(r)/max(S_D)$
10: $S_G(r) \leftarrow S_G(r)/max(S_G)$
11: $S(r) \leftarrow 0.4 * S_R(r) + 0.4 * S_D(r) + 0.2 * S_G(r)$
12: **if** $DHGM(r) = 1$ **then**
13: $S(r) \leftarrow \alpha * S(r)$
14: **end if**
15: **end for**
16: **return** S

In Algorithm 1, we first perform collision detection on all candidate reset points, discarding those candidate reset points that overlap with virtual objects or physical proxies (line 1). Then, we start calculating the score for each candidate reset point (lines 2-6). First, We obtain the RSM value of the candidate reset point as the RULA score S_R (line 3). As shown in Fig. 6a, the distance score S_D is set directly to the distance from the candidate reset point to the physical hand (line 4). Next, we calculate the value of the retargeting gain score S_G (line 5). As shown in Fig. 6b, S_G is the retargeting gain value between the virtual hand and the physical hand to the candidate reset point, calculated as shown in equation (3):

$$\begin{cases} G_A = \theta = arccos(\frac{U_v \cdot U_p}{\|U_v\| \cdot \|U_p\|})(\frac{180}{\pi}) \\ G_T = \max\left(\frac{\|U_p\|}{\|U_v\|}, \frac{\|U_v\|}{\|U_p\|}\right) \\ S_G = 0.5 * G_A^* + 0.5 * G_T^* \end{cases} \tag{3}$$

where U_p denotes the vector from the physical hand to the candidate reset point, U_v denotes the vector from the virtual hand to the candidate reset point, and θ is the angle between the two vectors. G_A^* and G_T^* denote the normalized angular gain value and translation gain value, respectively.

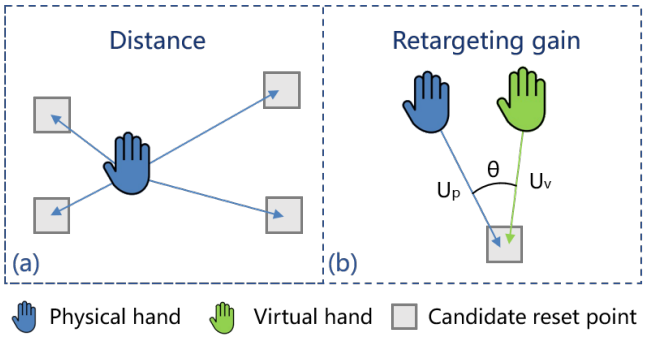

Fig. 6. (a) The distance score is the distance from the user's physical hand to the candidate reset point; (b) The retargeting gain is the translational gain and angular gain between the virtual hand and the physical hand to the candidate reset point in reset point selection

The three different scores correspond to the three design rationales in Section III (the RULA score for Ergonomics and Psychology, the distance score for Efficiency, and the retargeting gain score for Perception). Finally, we normalize all scores, max denotes the maximum value in a set of scores (lines 8-10). For each candidate reset point, we weight and sum the scores to obtain a final score (line 11). We use the $DHGM$ value of the candidate reset point to determine if it is in the dominant side area, and if so, multiplying the final score by the dominant hand gain value α. It is a value less than 1 and makes candidate reset points in the dominant side area have smaller scores and thus are more likely to be selected (lines 12-13).

D. Proxy and Placement Location Updating Algorithm

We present a proxy and placement location updating algorithm. The algorithm is introduced because the old physical proxy or placement may not be optimal after the reset, and we consider that the user's comfort should also be considered when selecting the physical proxy or placement location.

1) Physical proxy updating

The updating of physical proxies is performed if a reset occurs while picking up the virtual object with haptic retargeting. The algorithm is shown in Algorithm 2. Given Angle threshold A, Translation threshold T, Physical proxies $PList$, Virtual objects $VList$, Physical hand position H_p, Virtual hand position H_v, Selected virtual object P_v, the final score for each physical proxy S is calculated.

Algorithm 2 proxy updating algorithm based on comfort maps

Input: Angle threshold A, Translation threshold T, Physical proxies $PList$, Virtual objects $VList$, Physical hand position H_p, Virtual hand position H_v, Selected virtual object P_v

Output: Final score for each physical proxy S

1: **for** *each p in PList* **do**
2: $S_R(p) \leftarrow RSM(p)$
3: $S_I(p) \leftarrow 1/getImportance(p, VList)$
4: $S_G(p) \leftarrow getRetargetingGain(A, T, H_p, H_v, P_v, p)$
5: **end for**
6: **for** *each p in PList* **do**
7: $S_R(p) \leftarrow S_R(p)/max(S_R)$
8: $S_G(p) \leftarrow S_G(p)/max(S_G)$
9: $S_I(p) \leftarrow S_I(p)/max(S_I)$
10: $S(p) \leftarrow 0.4 * S_R(p) + 0.4 * S_I(p) + 0.2 * S_G(p)$
11: **end for**
12: **return** S

Picking up physical proxies has no collision problem, and we directly calculate the score for each physical proxy (lines 1-5). Firstly, we obtain the RSM value of the physical proxies as the RULA score S_R (line 2). Next, we calculate the importance score S_I. $getImportance$ calculates the importance of physical proxy or placement location, which is defined as the sum of the distances of a physical proxy to all other virtual objects, as shown in Fig. 7a, the smaller the sum of the distances of a physical proxy to the other virtual objects indicates that more virtual objects surround it, and its proxy capability is higher [28]. In proxy updating, the importance score calculation is $S_I(p) \leftarrow 1/getImportance(p, VList)$. This is because, we would like to take away physical proxies with lower importance (line 3). The retargeting gain score S_G is also calculated as shown in equation (3). As shown in Fig. 7b, here U_p denotes the vector from physical hand to physical proxy, U_v denotes the vector from virtual hand to virtual object, and θ is the angle between the two vectors (line 4). The three different scores correspond to the three design rationales in Section III (the RULA score for Ergonomics and Psychology, the importance score for Efficiency, and the retargeting gain score for Perception). We didn't use distance score and dominant hand gain in the updating algorithm. When selecting physical proxies and placement locations, it is not always better to be as close to the physical hand as possible. In addition, dominant hand gain is no longer applicable, which leads to the stacking of physical proxies on the dominant hand's side. It is not conducive to the global proxy for virtual objects. Finally, we normalize all scores (lines 7-9). For each physical proxy, we weight and sum the scores to obtain its final score (line 10).

2) Placement location updating

The updating of the placement location is performed if a reset occurs while placing the virtual object with haptic retargeting. The placement location updating algorithm is very similar to Algorithm 2, but there are some differences. The algorithm is shown in Algorithm 3.

First, collision detection is needed to avoid collision between two physical proxies before selecting placement locations (line 1). Second, instead of traversing the physical proxies, the algorithm traverses the candidate placement locations (lines 2-12). Like the candidate reset points, we grid the virtual plane with one candidate placement location every 0.15m, totaling 9*9=81 candidate placement locations. Last, the importance score S_I calculation was changed to $S_I(l) \leftarrow getImportance(l, VList)$, where l denotes the candidate placement locations (line 4). In proxy updating, we take away physical proxies with lower importance, while in placement location updating, we would like to place physical proxies in locations with higher importance. Placing a physical

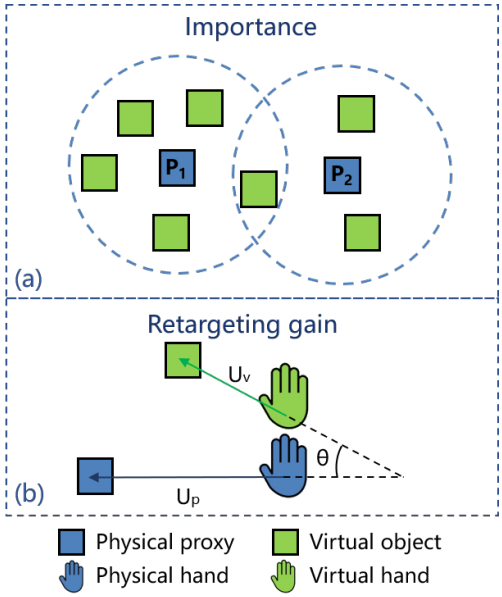

Fig. 7. (a) The importance score is used to measure the global proxy capability of a physical proxy. Physical proxy P_1 has more virtual objects around it than P_2, indicating that its global proxy capability is stronger; (b) The retargeting gain is translational gain and angular gain between virtual hand to virtual object and physical hand to physical proxy in proxy and placement updating

Algorithm 3 placement location updating algorithm based on comfort maps

Input: Angle threshold A, Translation threshold T, Candidate placement location $LList$, Virtual prop $VList$, Physical hand position H_p, Virtual hand position H_v, Selected virtual placement L_v

Output: Final score for each Candidate placement location S

1: $LList \leftarrow removeCollision(LList)$
2: **for** *each l in LList* **do**
3: $S_R(l) \leftarrow RSM(l)$
4: $S_I(l) \leftarrow getImportance(l, VList)$
5: $S_G(l) \leftarrow getRetargetingGain(A, T, H_p, H_v, L_v, l)$
6: **end for**
7: **for** *each l in LList* **do**
8: $S_R(l) \leftarrow S_R(l)/max(S_R)$
9: $S_G(l) \leftarrow S_G(l)/max(S_G)$
10: $S_I(l) \leftarrow S_I(l)/max(S_I)$
11: $S(l) \leftarrow 0.4 * S_R(l) + 0.4 * S_I(l) + 0.2 * S_G(l)$
12: **end for**
13: **return** S

proxy with low proxy capability to a location with high proxy capability can improve the global proxy capability of physical proxies and effectively reduce the number of resets [4]. Finally, we select the candidate placement location with the lowest score as the new placement location.

V. Pilot User Study: Determine Dominant hand gain value

In Section IV-A, we present the dominant hand gain map. When the user needs to perform a reset, we want the reset point to be on the user's dominant-hand side as much as possible. In this section, we will design a pilot user study to evaluate a reasonable value for the dominant hand gain value α. Fig. 8 shows a top view of the experimental scene with 10 randomly distributed green virtual objects and 5 evenly distributed blue physical proxies on a 1.5m*1.5m plane. The green star indicates the initial position of the user. The blue dashed line indicates the interaction boundary of our haptic retargeting method. The study has been approved by the Biology and Medical Ethics Committee of Beihang University.

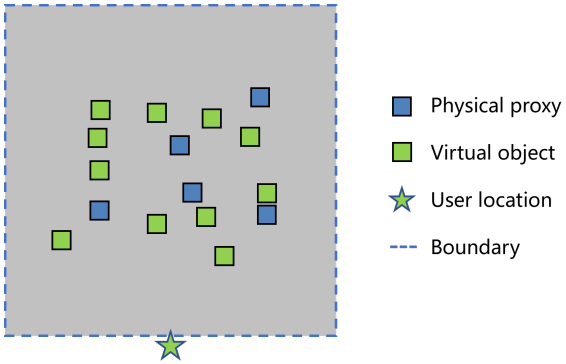

Fig. 8. Top view of the experimental scene, at the beginning, with blue physical proxies placed evenly throughout the scene.

A. User Study Design

Participant Twenty participants (14 males and 6 females; two of the participants are left-handed, and remaining participants are right-handed; aged 22–28, mean=24.1) from our university were recruited for this study. Among the participants, 15 of them had prior experience with VR applications. All participants had normal or corrected vision, and none of them reported any visual impairments or balance disorders.

Hardware setup We used the HTC VIVE system, which consists of tracked and positioned HMD and 6 trackers. The HMD was connected to a computer with an Intel i9-13900F processor, 64GB of RAM, and an RTX 4080 graphics card. Users wore the HMD on their heads during the experiments. The trackers are used to track the user's hand and the physical proxies and the HMD is used to track the user's body. Our experimental platform was implemented using Unity 2021.1.28f1c1. The prototype of our platform was built on the HaRT toolkit [39].

Task This study consisted of five sessions, and all participants were required to attend the five sessions. Each of the five sessions used our reset point optimization and proxy/placement location updating method but was given a different dominant hand gain value α: session 1 with $\alpha = 1$, session 2 with $\alpha = 0.9$, session 3 with $\alpha = 0.8$, session 4 with $\alpha = 0.6$ and session 5 with $\alpha = 0.4$. In selecting proxies and placement locations, we used the proxy importance method [4]. The order of the sessions was counterbalanced across participants. In each session, the participant is required to move the virtual cubes with the physical proxies 30 times. The system would generate a random string of numbers indicating the cube to be moved, and the system would highlight in red the current cube to be moved up to the number of interactions required to complete. When a virtual cube is picked up, the system generates a random location on the virtual plane and places a red cube to indicate the target location for placement. For a fair comparison, the virtual cube being manipulated and the corresponding placement location indicated by the system in the virtual scene were the same in all sessions. The initial position of the physical proxies and the distribution of the virtual objects at the start of the mission were also the same in all sessions. In addition, we asked the participants to try to keep their hands moving in a straight line without excess hand movements while performing the procedures.

Procedure Participants sat in front of a table where five physical cubes with trackers were placed. The physical cubes and table were aligned with the virtual world, and the virtual hand was aligned with the participant's real hand. If the retargeting exceeds the threshold, the participant needs to touch the reset point to complete the reset operation. The system would alert the participant by displaying a red "Need Reset" at the top of the virtual plane and showing the reset point in orange. Otherwise, the participant could continue the interaction without interruption. Before the entire study, we introduced participants to how to use our haptic retargeting method and gave them 5 minutes to familiarize themselves with the interaction. Before the experiment officially began, participants were required to complete 5 pick-and-place procedure exercises. We gave them a 2-minute break at the end of each session. It took each participant around 30 minutes to complete all tasks. The study metrics were recorded automatically during the tasks. In total, 5 (sessions) × 30 (pick-and-place procedures) × 20 (participants) =3000 procedures of data were collected.

Metrics The participants' task performance is measured using the following objective metrics:

- **Reset rate:** defined as the ratio of the number of retargeting trips involving resetting to the total number of retargeting trips;
- **Reset distance traveled & Reset time:** defined as the distance the user's hand traveled and the time spent while performing the reset operation;
- **Total distance traveled & Task completion time:** defined as the distance the user's hand traveled and the time spent while completing all 30 pick-and-place procedures;
- **RULA Score:** defined as the user's RULA score while performing a reset operation and picking up a physical proxy or placing a physical proxy after reset;
- **Dominant Hand Score:** defined as whether the reset point is set on the user's dominant side when the user performs the reset operation, and if it is on the user's dominant side, the score will be +1, and if it is not on the user's dominant side, the score will be +2.

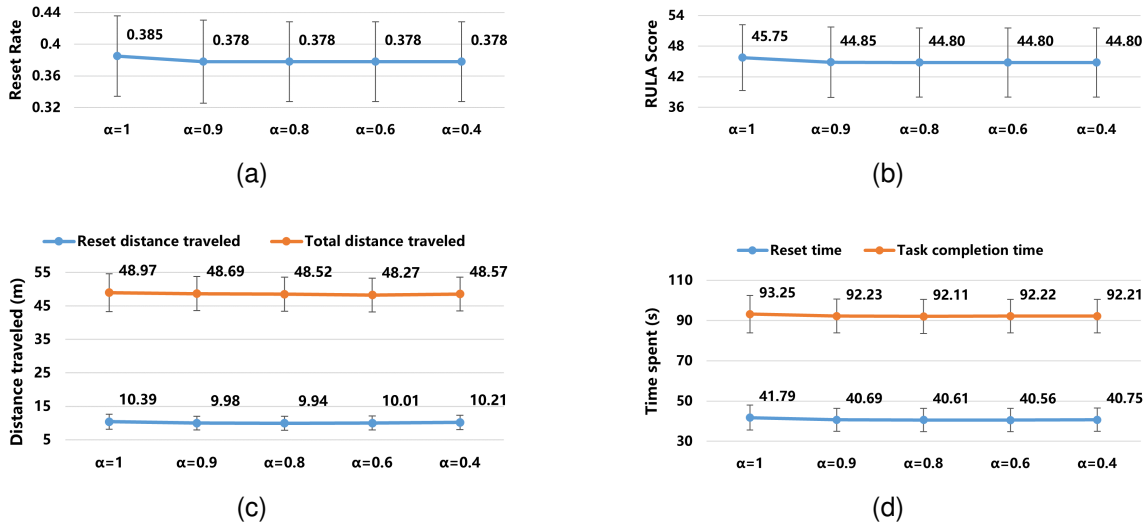

Fig. 9. (a) Mean Reset rate, (b) mean RULA Score, (c) mean Distance traveled, (d) mean Time spent of five sessions. Error bars indicate standard deviation.

B. Results

We performed statistics on all metrics for each session. The Shapiro-Wilk test [40] was used to assess the normality of the data distribution. Next, the assumption of sphericity was evaluated using Mauchly test [41], and if violated, Greenhouse-Geisser correction [42] was applied. Subsequently, RMANOVA [43] was conducted, followed by posthoc tests with Bonferroni-adjustment [44] to analyze the differences. p-values from the statistical tests to quantify the effect sizes were reported. The following are the results of the analysis.

Reset Rate No significant effect is found in the comparison of Session 1 vs Session 2 vs Session 3 vs Session 4 vs Session 5 ($F_{1.419,26.956} = 1.98, p = .167$), indicating that different dominant hand gain values have almost no effect on the number of resets. The slightly higher reset rate in Session 1 than in Sessions 2-4 may be due to a factor of chance. Fig. 9a shows the mean reset rate of the five sessions. Sessions 2-4 had the same mean reset rate of 0.378. Session 1 had the highest reset rate of 0.385, only 1.8% higher than Session 2-4.

Reset distance traveled & Reset time For both reset distance traveled and reset time, no significant effect is found in the comparison of Session 1 vs Session 2 vs Session 3 vs Session 4 vs Session 5 (Reset distance traveled: $F_{1.444,27.432} = 1.80, p = .190$; Reset time: $F_{1.295,24.606} = 3.08, p = .082$). Fig. 9c and Fig. 9d show the mean reset distance traveled and mean reset time of the five sessions, respectively. The difference in reset distance traveled and reset time for the 5 sessions is very small. For the Reset distance traveled, the maximum value (Session 1) is only 4.3% higher than the minimum value (Session 3), and for the Reset time, the maximum value (Session 1) is only 2.9% higher than the minimum value (Session 4).

Total distance traveled & Task completion time For both total distance traveled and task completion time, no significant effect is found in the comparison of Session 1 vs Session 2 vs Session 3 vs Session 4 vs Session 5 (Total distance traveled: $F_{1.217,23.118} = 0.64, p = .460$, Task completion time: $F_{1.048,19.913} = 1.965, p = .176$). Fig. 9c and Fig. 9d show the mean total distance traveled and mean task completion time of the five sessions, respectively. As with reset distance traveled and reset time, the difference in total distance traveled and task completion time for the 5 sessions is also very small.

RULA Score No significant effect is found in the comparison of Session 1 vs Session 2 vs Session 3 vs Session 4 vs Session 5 ($F_{1.261,23.966} = 2.48, p = .122$). Fig. 9b shows the mean RULA score for the five sessions. Sessions 3-5 have the same RULA score of 44.80. The maximum RULA score (Session 1) was only 2.1% higher than the minimum (Sessions 3-5).

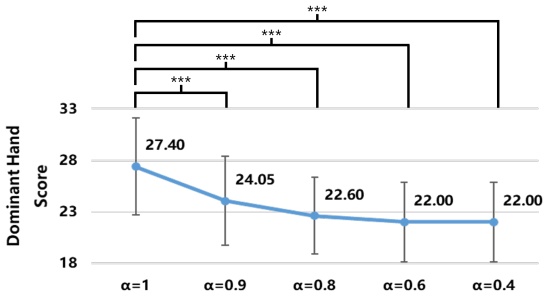

Fig. 10. Mean Dominant Hand Score of the five sessions. Error bars indicate standard deviation. Asterisks denote statistical significance. One star (*) denotes $0.01 < p < 0.05$, two stars (**) denotes $0.001 < p < 0.01$, three stars (***) denotes $p < 0.001$, and no stars denotes $p > 0.05$.

Dominant Hand Score Significant interaction effects are found in the comparison of Session 1 vs Session 2 vs Session 3 vs Session 4 vs Session 5 ($F_{1.750,33.251} = 76.48, p < .001$). In addition, significant interaction differences were found for sessions 1 vs 2 ($p < .001$), 1 vs 3 ($p < .001$), 1 vs 4 ($p < .001$), and 1 vs 5 ($p < .001$), indicating that the addition of the dominant hand gain does reduce the dominant hand score. No significant effect is found in the comparison of Session 2 vs Session 3 ($p = .263$) and Session 3 vs Session 4 ($p = .620$), indicating that the dominant hand score no longer changes significantly when the dominant hand gain value is reduced to a certain level. The dominant hand score

is the same for Session 4 and Session 5. Fig. 10 shows the mean dominant hand score of the five sessions. It can be seen that the dominant hand score decreases as the dominant hand gain value decreases. Session 5 shows a 24.5% decrease in dominant hand score compared to Session 1.

C. Discussion

Based on the above results, we found that the effect of the dominant hand gain on the reset rate, the distance traveled, the time spent, and the RULA score were all small. This is most likely because our dominant hand gain makes the final score smaller for candidate reset points on the dominant hand side. As long as the dominant hand gain value is within a reasonable range, the scores multiplied by the dominant hand gain value will still be large for candidate reset points that are farther away and have larger RULA scores. It won't cause our method to mis-select reset points that don't make sense.

As the dominant hand gain value decreases, the dominant hand score continues to decrease, indicating that the dominant hand gain value does allow the reset point to appear more on the user's dominant hand side to satisfy the user's psychological needs. In addition, when the value decreases to a certain degree, the dominant hand score no longer decreases significantly. From the results, the mean dominant hand score is the same when $\alpha = 0.4$ and $\alpha = 0.6$, indicating that both play the same role in selecting the reset point. Too small a value of α may lead to a mis-selection of the reset point, so we choose the largest value of α that minimizes the dominant hand score without affecting the other metrics. Ultimately, we choose $\alpha = 0.6$ as the dominant hand gain value.

VI. User Study: Evaluate our method

In this section, we design a user study to evaluate the performance of our method. We compare our method with state-of-the-art reset optimization methods [4], [6]. We use this study to prove that our method improves user efficiency and makes haptic retargeting more comfortable. The experimental scene is set up in the same way as in the pilot user study. The study has been approved by the Biology and Medical Ethics Committee of Beihang University.

A. User Study Design

Participants and Hardware setup Twenty participants (17 males and 3 females; two of the participants are left-handed, and remaining participants are right-handed, aged 20–37, mean=24.5) from our university were recruited for this study. In the interests of fairness and accuracy, none of them have participated the pilot user study. Among the participants, 12 of them had prior experience with VR applications. All participants had normal or corrected vision, and none of them reported any visual impairments or balance disorders. The hardware setup of this study was the same as pilot user study.

Task and procedure This study consisted of three control conditions: $CC1$, $CC2$ and $CC3$, and two experimental conditions: $EC1$ and $EC2$. All participants were required to attend the five conditions. We compared $EC1$ with $EC2$, $CC1$, $CC2$ and $CC3$ in a controlled within-subjects study. $CC1$ and $CC2$ use the point reset method and the threshold reset method of Matthews et al. [6], respectively, and proxies are selected based on the closest distance to the selected virtual object [3]. Placement location is then determined by minimizing the sum of the distances of the proxies to all virtual objects [28]. $CC3$ is the method of Ziming et al [4]. The reset point is placed at the corner of the desktop on the user's dominant side. $EC1$ used our method with reset point optimization and proxy/placement location updating. $EC2$ used our method with only reset point optimization. In selecting proxies and placement locations, $EC1$ and $EC2$ used the framework of proxy importance based haptic retargeting method [4]. The order of the conditions was counterbalanced across participants.

The tasks and procedures of the study were the same as those of the pilot user study and will not be repeated here. It took each participant around 45 minutes to complete all tasks. The study metrics were recorded automatically during the tasks. After each task, we asked users to complete the NASA-TLX questionnaire. In total, 5 (conditions) × 30 (pick-and-place procedures) × 20 (participants) =3000 procedures of data were collected.

Metrics The objective metrics measuring participants' task completion were the same as in the pilot user study. In addition, we measure user task load to assess the VR experience. User task load is measured using NASA's standardized TLX questionnaire [45], which consists of six questions: Mental Demand, Physical Demand, Temporal Demand, Performance, Effort, and Frustration.

B. Results

We performed statistics on all metrics for each condition. The data were first evaluated for outliers using box plots, and any outliers were removed. Then, the Shapiro-Wilk test [40] was used to assess the normality of the data distribution. Next, the assumption of sphericity was evaluated using Mauchly test [41], and if violated, Greenhouse-Geisser correction [42] was applied. Subsequently, RMANOVA [43] was conducted, followed by posthoc tests with Bonferroni-adjustment [44] to analyze the differences. p-values from the statistical tests and Cohen's d [46] to quantify the effect sizes were reported. Cohen's d values were translated to qualitative effect size estimates of Huge ($d > 2.0$), Very Large ($2.0 > d > 1.2$), Large ($1.2 > d > 0.8$), Medium ($0.8 > d > 0.5$), Small ($0.5 > d > 0.2$), and Very Small ($0.2 > d$).

Reset Rate TABLE I gives the reset rate for the five conditions. A significant interaction effect is found in the comparison of EC1 vs EC2 VS CC1 vs CC2 vs CC3 ($F_{1.481,28.143} = 182.494, p < .001$), indicating that different methods of haptic retargeting have a significant effect on reset rate.

CC1 and CC2 have the same reset rate because they use the same proxy/placement location selection algorithm. ditto for EC2 and CC3. A significant interaction effect is found in the comparison of EC1 vs CC1/CC2 ($p < .001$), indicating that the proxy importance method can reduce the number of resets significantly. No significant effect is found in the comparison of EC1 vs EC2/CC3 ($p = .107$), but the reset rate of EC is 7.1% higher than that of EC2/CC3. This may be because

TABLE I
RESET RATE (%)

Condition	Avg ± std. dev.	$(*C_i$-$EC_1)$ / $*C_i$	p	Cohen's d	Effect size
$EC1$	0.36 ± 0.05				
$EC2$	0.34 ± 0.04	-7.1%	0.107	0.5	Medium
$CC1$	0.54 ± 0.04	32.2%	$< 0.001^*$	3.8	Huge
$CC2$	0.54 ± 0.04	32.2%	$< 0.001^*$	3.8	Huge
$CC3$	0.34 ± 0.04	-7.1%	0.107	0.5	Medium

our proxy/placement location updating algorithm considers more factors, such as comfort and retargeting gain, when performing the updating. This leads us to weaken its global proxy capability when updating proxies/placement locations. However, the impact on the reset rate is insignificant.

Reset distance traveled & Reset time TABLE II and TABLE III give the reset distance traveled and reset time for the five conditions, respectively. For both reset distance traveled and reset time, significant interaction effects are found in the comparisons of EC1 vs EC2 vs CC1 vs CC2 vs CC3 (Reset distance traveled: $F_{1.653,31.416} = 254.131, p < .001$, Reset time: $F_{1.477,28.062} = 265.192, p < .001$), indicating that the different methods of haptic retargeting have significant effects on both reset distance traveled and reset time.

TABLE II
RESET DISTANCE TRAVELED (M)

Condition	Avg ± std. dev.	$(*C_i$-$EC_1)$ / $*C_i$	p	Cohen's d	Effect size
$EC1$	9.56 ± 2.13				
$EC2$	10.87 ± 2.64	12.1%	0.099	0.5	Medium
$CC1$	39.45 ± 6.24	75.8%	$< 0.001^*$	6.4	Huge
$CC2$	36.67 ± 6.73	73.9%	$< 0.001^*$	5.4	Huge
$CC3$	31.70 ± 5.46	69.8%	$< 0.001^*$	5.3	Huge

TABLE III
RESET TIME (S)

Condition	Avg ± std. dev.	$(*C_i$-$EC_1)$ / $*C_i$	p	Cohen's d	Effect size
$EC1$	39.14 ± 5.97				
$EC2$	39.17 ± 5.99	0.1%	0.989	0.004	Very Small
$CC1$	91.64 ± 10.31	57.3%	$< 0.001^*$	6.2	Huge
$CC2$	87.96 ± 11.38	55.5%	$< 0.001^*$	5.3	Huge
$CC3$	66.83 ± 9.69	41.4%	$< 0.001^*$	3.4	Huge

For reset distance traveled, EC1 is significantly lower than CC1, CC2, and CC3 (all $p < .001$), because our method dynamically adjusts the position of the reset point to reduce the reset distance, and our total number of resets is lower. For reset time, EC1 is also significantly lower than CC1, CC2, and CC3 (all $p < .001$), this may partly because the distance traveled is smaller and partly because our method is more in line with people's ergonomic and psychological needs and the interaction is smoother with less thinking time. No significant effect is found in the comparison of EC1 vs EC2 (Reset distance traveled: $p = .099$, Reset time: $p = .989$) because both conditions use our reset point optimization algorithm.

Total distance traveled & Task completion time TABLE IV and TABLE V give the total distance traveled and task completion time for the five conditions, respectively. For both total distance traveled and task completion time, significant interaction effects are found in the comparisons of EC1 vs EC2 vs CC1 vs CC2 vs CC3 (Total distance traveled: $F_{1.578,29.982} = 225.775, p < .001$, Task completion time: $F_{1.478,28.083} = 242.577, p < .001$), indicating that the different methods of haptic retargeting have significant effects on both reset distance traveled and reset time.

TABLE IV
TOTAL DISTANCE TRAVELED (M)

Condition	Avg ± std. dev.	$(*C_i$-$EC_1)$ / $*C_i$	p	Cohen's d	Effect size
$EC1$	47.73 ± 5.33				
$EC2$	51.02 ± 5.66	5.4%	0.073	0.6	Medium
$CC1$	94.05 ± 12.73	49.2%	$< 0.001^*$	4.7	Huge
$CC2$	98.62 ± 14.08	51.6%	$< 0.001^*$	4.8	Huge
$CC3$	90.21 ± 10.14	47.1%	$< 0.001^*$	5.2	Huge

TABLE V
TASK COMPLETION TIME (S)

Condition	Avg ± std. dev.	$(*C_i$-$EC_1)$ / $*C_i$	p	Cohen's d	Effect size
$EC1$	90.13 ± 8.99				
$EC2$	92.89 ± 9.36	3.0%	0.359	0.3	Small
$CC1$	164.47 ± 18.49	45.2%	$< 0.001^*$	5.1	Huge
$CC2$	170.69 ± 20.63	47.2%	$< 0.001^*$	5.1	Huge
$CC3$	145.27 ± 15.99	37.9%	$< 0.001^*$	4.3	Huge

As with Reset distance traveled & Reset time, both metrics are significantly lower for EC1 than for CC1, CC2, and CC3 (all $p < .001$). This may be partly because EC1's reset distance traveled and reset time are inherently less and partly because our method sets the reset point and the proxy/placement location in places that are more in line with people's ergonomic and psychological needs. Still, no significant effect is found in the comparison between EC1 and EC2 (Total distance traveled: $p = .073$, Task completion time: $p = .359$).

RULA score TABLE VI gives the RULA score for the five conditions. A significant interaction effect is found in the comparison of EC1 vs EC2 vs CC1 vs CC2 vs CC3 ($F_{1.625,30.880} = 551.886, p < .001$), indicating that different methods of haptic retargeting have a significant effect on RULA Score.

TABLE VI
RULA SCORE

Condition	Avg ± std. dev.	$(*C_i$-$EC_1)$ / $*C_i$	p	Cohen's d	Effect size
$EC1$	44.10 ± 6.08				
$EC2$	51.85 ± 7.37	14.9%	$0.001*$	1.2	Very Large
$CC1$	103.90 ± 8.28	57.6%	$< 0.001^*$	8.2	Huge
$CC2$	108.25 ± 9.92	59.3%	$< 0.001^*$	7.8	Huge
$CC3$	68.65 ± 9.24	35.8%	$< 0.001^*$	3.1	Huge

Significant effects are found in the comparisons of EC1 vs CC1, EC1 vs CC2, and EC1 vs CC3 (all $p < .001$), indicating that our method can set the reset point in the area with lower RULA scores and update the proxy/placement location to a more reasonable position to allow users to interact in a more comfortable manner. A significant effect is also found in the comparison of EC1 vs EC2 ($p = .001$), demonstrating the effectiveness of the proxy/placement location updating algorithm, which can further reduce the user's RULA score.

Dominant hand score TABLE VII gives the dominant hand score for the five conditions. A significant interaction effect is found in the comparison of EC1 VS EC2 vs CC1 vs CC2 vs CC3 ($F_{1.888,35.870} = 223.748, p < .001$), indicating that different methods of haptic retargeting have a significant effect on dominant hand score.

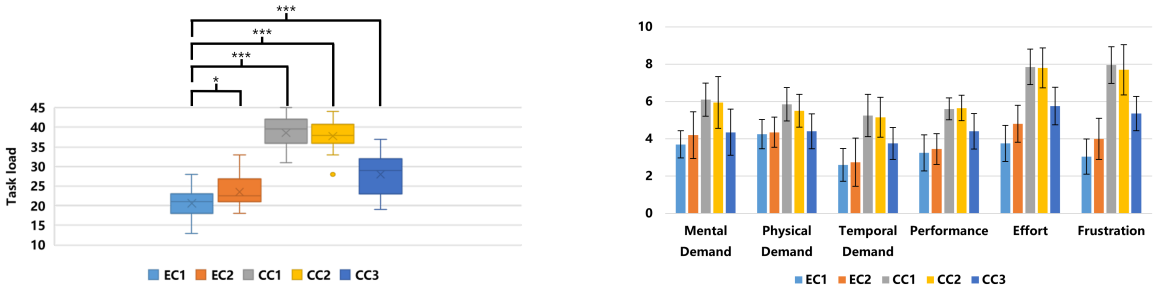

Fig. 11. (a) Box plots for Task load scores for all conditions, (b) mean score of each NASA-TLX dimension. Error bars indicate standard deviation. Asterisks denote statistical significance.

TABLE VII
DOMINANT HAND SCORE

Condition	Avg $\pm$ std. dev.	$(*C_i\text{-}EC_1)$ / $*C_i$	p	Cohen's d	Effect size
$EC1$	21.45 ± 3.31				
$EC2$	21.90 ± 3.65	2.1%	0.693	0.1	Very Small
$CC1$	38.80 ± 3.52	44.7%	$< 0.001^*$	8.2	Huge
$CC2$	37.90 ± 3.73	43.4%	$< 0.001^*$	7.8	Huge
$CC3$	17.35 ± 2.13	-23.6%	$< 0.001^*$	1.4	Very Large

Significant effects are found in the comparisons of EC1 vs CC1 and EC1 vs CC2 (all $p < .001$), indicating that our dominant hand gain can set the reset point more on the side of the user's dominant hand. A significant effect is also found in the comparison of EC1 vs CC3 ($p < .001$), but the CC3 has a higher dominant hand score than the EC1. This is because the CC3 method fixed the reset point at the corner of the table on the side of the user's dominant hand. The dominant hand scores of EC1 and EC2 are almost the same ($p = .693$), with a difference of only 2.1%, and both conditions use our reset point optimization algorithm, which can satisfy the user's psychological needs.

Task load Fig. 11a shows the Task load scores for all conditions. A significant interaction effect is found in the comparison of EC1 vs EC2 vs CC1 vs CC2 vs CC3 ($F_{2.734,51.947} = 114.783, p < .001$), indicating that different methods of haptic retargeting have a significant effect on task load. Our method can significantly reduce the task load compared to the methods of Matthews et al. [6] (EC1 vs CC1: $p < .001$, EC1 vs CC2: $p < .001$) and Ziming et al. [4] (EC1 vs CC3: $p < .001$). No significant effect is found in the comparison of CC1 and CC2 ($p = 0.479$), and the task load of both CC1 and CC2 is high. A significant effect is also found in the comparison of EC1 vs EC2 ($p = 0.023$), indicating that our proxy/placement location updating algorithm can further improve the user experience.

Fig. 11b shows the mean scores of each NASA-TLX dimension. EC1 method is the most preferred in all dimensions. For 'Mental Demand', 'Physical Demand', 'Temporal Demand', 'Effort' and 'Frustration', CC1's method is the least preferred. For 'Performance', CC2's method is the least preferred. This may be because the CC1 and CC2 methods may not be suitable for highly dynamic haptic retargeting scenarios. Moreover, both methods do not consider the user's comfort and have a higher number of resets. This will undoubtedly seriously affect the user experience. 'Mental Demand', 'Effort', and 'Frustration' can reflect the user's comfort and EC1 method is apparently the most comfortable for the user.

C. Discussion

We compare our method with state-of-the-art haptic retargeting reset optimization methods [4], [6].

Compared to Ziming et al.'s method [4], our method slightly increases the number of resets, but the increase is only 7.1%. For the metrics of reset distance traveled, reset time, total distance traveled, and task completion time, our method is much better than Ziming et al.'s method in test scenario because we dynamically set the reset point near the user's physical hand, reducing the extra hand movement. For RULA scores, our method is significantly better than Ziming et al.'s method. Our reset point optimization algorithm always sets the reset point in the area with lower RULA scores, and the updating algorithm also guides the user to pick up or place physical proxies in the area with lower RULA scores. For the dominant hand score, Ziming et al.'s method is lower than ours because their method fixes the reset point at the corner of the table on the side of the user's dominant hand, which must satisfy the psychological needs of the dominant hand every time. Our method, on the other hand, in addition to considering the needs of the dominant hand, also needs to consider a number of indicators such as distance, retargeting gain, and RULA score.

Compared to Matthews et al.'s method [6], our reset rate is lower because we use the proxy importance method for the selection of physical proxies and placement locations. For the metrics of reset distance traveled, reset time, total distance traveled and task completion time, our method is also much better than Matthews et al.'s method. On the one hand, it is because our reset times are much lower, and on the other hand, the distance traveled for a single reset in our method is much lower than theirs (The smaller the value of "reset distance traveled/reset rate" the smaller the distance traveled for a single reset. ours: $9.56/0.36 = 26.6$, point reset: $39.45/0.54 = 73.1$, threshold reset: $36.67/0.54 = 67.9$). For the RULA score and dominant hand score, our method also outperforms the method of Matthews et al. Because their method does not consider the user's comfort when setting the reset position, they only consider the effect of distance and retargeting gain.

VII. Conclusion, Limitations, and Future work

In this paper, we have proposed a reset point optimization algorithm and a proxy and placement location updating algorithm. The reset point optimization algorithm allows the user to perform the reset operation quickly and comfortably, while the proxy and placement location updating algorithm re-selects a more reasonable proxy or placement location when a reset occurs. For the first time, we have introduced the influence of ergonomics and psychology into the haptic retargeting method. Compared to state-of-the-art methods, our method can improve efficiency by significantly reducing the user's hand movements. In addition, the results of RULA score, dominant hand score, and NASA-TLX questionnaire indicate that our method does satisfy users' ergonomic and psychological needs and makes the user more comfortable during the haptic retargeting interaction.

We have proven the superiority of our method in terms of efficiency and comfort, but it still has some limitations. First, our method assumes that the user is not moving and that the size of the table is comparable to the reachable range of the user's arm. This is the most common scenario for haptic retargeting, e.g., playing chess or building blocks. Our method may not work well for scenes that are too small or too large. Second, our method remains scripted when conducting user experiments, which means that users can only follow the order predetermined by the system. Third, our method has excellent performance in test scenario, but more application scenarios are yet to be tested. Fourth, we build $DHGM$ with the palm facing down by default, without taking into account the rotation of the hand. Finally, our method only considers 2D plane positions and does not consider height variations.

In the future, we will consider the impact of user walking on the range of manipulation and comfort and combine redirected walking with haptic retargeting. Second, we will support unscripted interaction through gaze point selection or neural network prediction to improve the user's interaction freedom. Third, we will demonstrate the generality of our method to other scenarios and settings. Fourth, we will weight $DHGM$ in different directions to get a more refined map. Finally, we will extend our method to 3D space to further expand its application scenarios.

Acknowledgments

This work was supported by the National Natural Science Foundation of China under Grant 61932003, under Grant 62372026, in part by the Beijing Science and Technology Plan Project under Grant Z221100007722004, and in part by the National Key R&D plan under Grant 2019YFC1521102.

References

[1] M. Azmandian, M. Hancock, H. Benko, E. Ofek, and A. D. Wilson, "Haptic retargeting: Dynamic repurposing of passive haptics for enhanced virtual reality experiences," in *Proceedings of the 2016 chi conference on human factors in computing systems*, 2016, pp. 1968–1979.

[2] L.-P. Cheng, E. Ofek, C. Holz, H. Benko, and A. D. Wilson, "Sparse haptic proxy: Touch feedback in virtual environments using a general passive prop," in *Proceedings of the 2017 CHI Conference on Human Factors in Computing Systems*, 2017, pp. 3718–3728.

[3] B. J. Matthews and R. T. Smith, "Head gaze target selection for redirected interaction," in *SIGGRAPH Asia 2019 XR*, 2019, pp. 13–14.

[4] Z. Liu, J. Wu, L. Wang, X. Li, and S. K. Im, "Proxy importance based haptic retargeting with multiple props in vr," *IEEE Transactions on Visualization and Computer Graphics*, 2024.

[5] B. J. Matthews, B. H. Thomas, S. Von Itzstein, and R. T. Smith, "Remapped physical-virtual interfaces with bimanual haptic retargeting," in *2019 IEEE Conference on Virtual Reality and 3D User Interfaces (VR)*. IEEE, 2019, pp. 19–27.

[6] B. J. Matthews, B. H. Thomas, G. S. Von Itzstein, and R. T. Smith, "Adaptive reset techniques for haptic retargeted interaction," *IEEE Transactions on Visualization and Computer Graphics*, vol. 29, no. 2, pp. 1478–1490, 2021.

[7] H. Iwata, H. Yano, F. Nakaizumi, and R. Kawamura, "Project feelex: adding haptic surface to graphics," in *Proceedings of the 28th annual conference on Computer graphics and interactive techniques*, 2001, pp. 469–476.

[8] K. R. Vaghela, A. Trockels, and M. Carobene, "Active vs passive haptic feedback technology in virtual reality arthroscopy simulation: Which is most realistic?" *Journal of Clinical Orthopaedics and Trauma*, vol. 16, pp. 249–256, 2021.

[9] W. A. McNeely, "Robotic graphics: a new approach to force feedback for virtual reality," in *Proceedings of IEEE Virtual Reality Annual International Symposium*. IEEE, 1993, pp. 336–341.

[10] B. E. Insko, *Passive haptics significantly enhances virtual environments*. The University of North Carolina at Chapel Hill, 2001.

[11] N. C. Nilsson, A. Zenner, and A. L. Simeone, "Propping up virtual reality with haptic proxies," *IEEE Computer Graphics and Applications*, vol. 41, no. 5, pp. 104–112, 2021.

[12] J. J. Gibson, "Adaptation, after-effect and contrast in the perception of curved lines." *Journal of experimental psychology*, vol. 16, no. 1, p. 1, 1933.

[13] E. Burns, S. Razzaque, A. T. Panter, M. C. Whitton, M. R. McCallus, and F. P. Brooks, "The hand is slower than the eye: A quantitative exploration of visual dominance over proprioception," in *IEEE Proceedings. VR 2005. Virtual Reality, 2005.* IEEE, 2005, pp. 3–10.

[14] B. J. Matthews, C. Reichherzer, and R. T. Smith, "Remapped interfaces: Building contextually adaptive user interfaces with haptic retargeting," in *Extended Abstracts of the 2023 CHI Conference on Human Factors in Computing Systems*, 2023, pp. 1–4.

[15] A. Zenner, K. P. Regitz, and A. Krüger, "Blink-suppressed hand redirection," in *2021 IEEE Virtual Reality and 3D User Interfaces (VR)*. IEEE, 2021, pp. 75–84.

[16] A. Zenner, C. Karr, M. Feick, O. Ariza, and A. Krüger, "Beyond the blink: Investigating combined saccadic & blink-suppressed hand redirection in virtual reality," in *Proceedings of the CHI Conference on Human Factors in Computing Systems*, 2024, pp. 1–14.

[17] R. A. Montano Murillo, S. Subramanian, and D. Martinez Plasencia, "Erg-o: Ergonomic optimization of immersive virtual environments," in *Proceedings of the 30th annual ACM symposium on user interface software and technology*, 2017, pp. 759–771.

[18] A. L. Simeone, E. Velloso, and H. Gellersen, "Substitutional reality: Using the physical environment to design virtual reality experiences," in *Proceedings of the 33rd Annual ACM Conference on Human Factors in Computing Systems*, 2015, pp. 3307–3316.

[19] X. de Tinguy, C. Pacchierotti, M. Marchal, and A. Lécuyer, "Toward universal tangible objects: Optimizing haptic pinching sensations in 3d interaction," in *2019 IEEE Conference on Virtual Reality and 3D User Interfaces (VR)*. IEEE, 2019, pp. 321–330.

[20] J. Yang, H. Horii, A. Thayer, and R. Ballagas, "Vr grabbers: Ungrounded haptic retargeting for precision grabbing tools," in *Proceedings of the 31st Annual ACM Symposium on User Interface Software and Technology*, 2018, pp. 889–899.

[21] H.-Y. Huang, C.-W. Ning, P.-Y. Wang, J.-H. Cheng, and L.-P. Cheng, "Haptic-go-round: A surrounding platform for encounter-type haptics in virtual reality experiences," in *Proceedings of the 2020 CHI Conference on Human Factors in Computing Systems*, 2020, pp. 1–10.

[22] M. Hoppe, P. Knierim, T. Kosch, M. Funk, L. Futami, S. Schneegass, N. Henze, A. Schmidt, and T. Machulla, "Vrhapticdrones: Providing haptics in virtual reality through quadcopters," in *Proceedings of the 17th International Conference on Mobile and Ubiquitous Multimedia*, 2018, pp. 7–18.

[23] P. Abtahi, B. Landry, J. Yang, M. Pavone, S. Follmer, and J. A. Landay, "Beyond the force: Using quadcopters to appropriate objects and the environment for haptics in virtual reality," in *Proceedings of the 2019 CHI Conference on Human Factors in Computing Systems*, 2019, pp. 1–13.

[24] A. Clarence, J. Knibbe, M. Cordeil, and M. Wybrow, "Unscripted retargeting: Reach prediction for haptic retargeting in virtual reality,"

in *2021 IEEE Virtual Reality and 3D User Interfaces (VR)*. IEEE, 2021, pp. 150–159.
[25] M. Salvato, N. Heravi, A. M. Okamura, and J. Bohg, "Predicting hand-object interaction for improved haptic feedback in mixed reality," *IEEE Robotics and Automation Letters*, vol. 7, no. 2, pp. 3851–3857, 2022.
[26] M. Feick, K. P. Regitz, A. Tang, T. Jungbluth, M. Rekrut, and A. Krüger, "Investigating noticeable hand redirection in virtual reality using physiological and interaction data," in *2023 IEEE Conference Virtual Reality and 3D User Interfaces (VR)*. IEEE, 2023, pp. 194–204.
[27] Y. Zhao and S. Follmer, "A functional optimization based approach for continuous 3d retargeted touch of arbitrary, complex boundaries in haptic virtual reality," in *Proceedings of the 2018 CHI Conference on Human Factors in Computing Systems*, 2018, pp. 1–12.
[28] X. Yang, Y. Kang, and X. Yang, "Retargeting destinations of passive props for enhancing haptic feedback in virtual reality," in *2022 IEEE Conference on Virtual Reality and 3D User Interfaces Abstracts and Workshops (VRW)*. IEEE, 2022, pp. 618–619.
[29] A. Zenner and A. Krüger, "Estimating detection thresholds for desktop-scale hand redirection in virtual reality," in *2019 IEEE Conference on Virtual Reality and 3D User Interfaces (VR)*. IEEE, 2019, pp. 47–55.
[30] A. Clarence, J. Knibbe, M. Cordeil, and M. Wybrow, "Investigating the effect of direction on the limits of haptic retargeting," in *2022 IEEE International Symposium on Mixed and Augmented Reality (ISMAR)*. IEEE, 2022, pp. 612–621.
[31] N. Ogawa, T. Narumi, and M. Hirose, "Effect of avatar appearance on detection thresholds for remapped hand movements," *IEEE transactions on visualization and computer graphics*, vol. 27, no. 7, pp. 3182–3197, 2020.
[32] B. Benda, S. Esmaeili, and E. D. Ragan, "Determining detection thresholds for fixed positional offsets for virtual hand remapping in virtual reality," in *2020 IEEE International Symposium on Mixed and Augmented Reality (ISMAR)*. IEEE, 2020, pp. 269–278.
[33] L. McAtamney and E. N. Corlett, "Rula: a survey method for the investigation of work-related upper limb disorders," *Applied ergonomics*, vol. 24, no. 2, pp. 91–99, 1993.
[34] D. Casasanto and E. G. Chrysikou, "When left is "right" motor fluency shapes abstract concepts," *Psychological science*, vol. 22, no. 4, pp. 419–422, 2011.
[35] R. Daini, G. Vallar, and L. S. Arduino, "Why we move to the right? the dominant hand motor-spatial bias." *Journal of Experimental Psychology: General*, vol. 147, no. 10, p. 1488, 2018.
[36] P. J. Rowe, C. Haenschel, M. Kosilo, and K. Yarrow, "Objects rapidly prime the motor system when located near the dominant hand," *Brain and cognition*, vol. 113, pp. 102–108, 2017.
[37] M. Steele and T. Chenier, "Arm-span, height, and age in black and white women," *Annals of human biology*, vol. 17, no. 6, pp. 533–541, 1990.
[38] P. H. Quanjer, A. Capderou, M. M. Mazicioglu, A. N. Aggarwal, S. D. Banik, S. Popovic, F. A. Tayie, M. Golshan, M. S. Ip, and M. Zelter, "All-age relationship between arm span and height in different ethnic groups," *European Respiratory Journal*, vol. 44, no. 4, pp. 905–912, 2014.
[39] A. Zenner, H. M. Kriegler, and A. Krüger, "Hart-the virtual reality hand redirection toolkit," in *Extended Abstracts of the 2021 CHI Conference on Human Factors in Computing Systems*, 2021, pp. 1–7.
[40] N. M. Razali, Y. B. Wah *et al.*, "Power comparisons of shapiro-wilk, kolmogorov-smirnov, lilliefors and anderson-darling tests," *Journal of statistical modeling and analytics*, vol. 2, no. 1, pp. 21–33, 2011.
[41] S. S. Shapiro and M. B. Wilk, "An analysis of variance test for normality (complete samples)," *Biometrika*, vol. 52, no. 3-4, pp. 591–611, 1965.
[42] S. W. Greenhouse and S. Geisser, "On methods in the analysis of profile data," *Psychometrika*, vol. 24, no. 2, pp. 95–112, 1959.
[43] L. St, S. Wold *et al.*, "Analysis of variance (anova)," *Chemometrics and intelligent laboratory systems*, vol. 6, no. 4, pp. 259–272, 1989.
[44] J. D. Brown, "The bonferroni adjustment," *Statistics*, vol. 12, no. 1, pp. 23–27, 2008.
[45] S. G. Hart, "Nasa-task load index (nasa-tlx); 20 years later," in *Proceedings of the human factors and ergonomics society annual meeting*, vol. 50, no. 9. Sage publications Sage CA: Los Angeles, CA, 2006, pp. 904–908.
[46] J. Cohen, *Statistical power analysis for the behavioral sciences*. Routledge, 2013.

Aoxin Sun is a M.A student in the School of Computer Science and Engineering of Beihang University, China. His current research focuses on virtual reality, augmented reality and visualization.

Jian Wu received his Ph.D. degree from the State Key Laboratory of Virtual Reality Technology and Systems, School of Computer Science and Engineering, Beihang University, Beijing, China. He is currently an assistant professor at the School of Computer Science and Engineering, Beihang University, Beijing, China. His current research focuses on virtual reality, augmented reality, human-computer interaction and visualization.

Runze Fan is a Ph.D student at the School of Computer Science and Engineering, Beihang University, China. His current research focuses on virtual reality and augmented reality.

Sio Kei Im received his Ph.D. degree in Electronic Engineering from Queen Mary University of London (QMUL), United Kingdom. He is a professor at the Faculty of Applied Sciences, Macau Polytechnic University, and a researcher at the Engineering Research Center of Applied Technology on Machine Translation and Artificial Intelligence, Ministry of Education. His research interests include video coding, image processing, machine learning for NLP and multimedia.

Lili Wang received her Ph.D. degree from the Beihang University, Beijing, China. She is a professor with the School of Computer Science and Engineering of Beihang University, and a researcher with the State Key Laboratory of Virtual Reality Technology and Systems. Her interests include virtual reality, augmented reality, mixed reality, real-time rendering and realistic rendering.